Journal of Ultrafine Grained and Nanostructured Materials
Ultrafine Grained and Nanostructured Materials

Journal of Ultrafine Grained and Nanostructured Materials
https://jufgnsm.ut.ac.ir
Vol. 58, No.1, June 2025, pp. 25-32
Print ISSN: 2423-6845 Online ISSN: 2423-6837
DOI: 10.22059/jufgnsm.2025.01.03

Porous Carbon Grain from Coconut Shell Biochar for Permeable Composite Paver

Cindy Mutiara Septani[1,3a*], Faidliyah Nilna Minah[1b], M. Istnaeny Hudha[1c], Mohammad Erfan[2d]

[1]Department of Chemical Engineering, Institut Teknologi Nasional Malang, Indonesia
[2]Department of Civil Engineering, Institut Teknologi Nasional Malang, Indonesia
[3]Research Center for Polymer Technology, National Research and Innovation Agency, South Tangerang, Indonesia

Recieved: 17 January 2025; Accepted: 10 April 2025

[*]Corresponding author, E-mail: cindymutiara13@lecturer.itn.ac.id, cindy.mutiara.septani@brin.go.id

ABSTRACT

Indonesia is one of the world's largest producers of agricultural commodities and waste. The abundance of agricultural waste releases CO_2 into the atmosphere and contributes to global warming and climate change. Carbon sequestration is one of the applicable and low-cost technologies to achieve sustainability and net zero emission. Here, we studied the coconut shell biochar as a composite material for a permeable paving block as an alternative to carbon sequestration. The novelty of this study elaborates on the direct connection between coconut-shell biochar, pyrolysis temperature, and its application as the paving block based on its chemical and physical properties. The pyrolysis temperature of the coconut shell biochar was varied at 400°C and 500°C to obtain biochar with the highest porosity. Biochar pyrolyzed at 500°C possesses the highest porosity with the surface-active area of 32.565 m^2/g. Composite pavers were fabricated by mixing the water, fine aggregates, Portland cement, and varied percentages of the ball-milled biochar pyrolyzed at 500°C. The increasing percentage of biochar increases water permeability. Inversely, the increase in biochar percentage reduces the compressive strength. The results show that $B_{20\%}$ which consists of 20% biochar is adequate to be utilized as a grade B paving block based on The Indonesian National Standard (SNI) 03-0691-1996. At $B_{20\%}$, the compression strength is 24.7 MPa and the water permeability is 6%.

Keywords: *biochar, carbon, porous material, grain, paver.*

1. Introduction

In recent years, the effect of climate change on our lives has become more prominent and severe. The global average temperature of the earth rises to an alarming degree, marking the new era of global boiling in 2023 [1], [2], [3]. The increasing concentration of greenhouse gases such as CO_2 in the atmosphere is the main trigger of climate change. This situation urgently calls for immediate action to reduce carbon footprints by utilizing a sustainable and net zero emission approach in agriculture, energy, transportation, industry, and technology fields [1], [2], [4], [5].

Indonesia is one of the world's largest producers of agricultural commodities. Agricultural products have become one of the main economic sectors in Indonesia. The large production of agricultural products results in enormous amounts of biomass waste. The poor regulation of biomass waste and technology limitations cause major environmental issues [2], [6], [7]. The abundance of untreated agricultural waste releases CO_2 into the atmosphere and contributes to the increase in global average temperature if the waste is not treated properly [8], [9], [10]. Carbon sequestration is one of the applicable and low-cost technologies to achieve sustainability and net zero emission. Carbon sequestration is the process of storing carbon in carbon storage to prohibit its release into the atmosphere for a long time. Mostly, the carbon is stored in the soil or deep inside the earth's layers. Carbon sequestration is also an act of carbon neutrality, which means that the stored carbon creates a balance between CO_2 in the atmosphere and in the soil, thus has no contribution to climate change [8], [9], [10].

Converting biomass waste into biochar is an alternative to carbon sequestration methods. Biochar is a carbon-rich solid material resulting from the conversion of agricultural biomass, such as coconut shells, corn cob, wood chips, etc., through incomplete combustion with a limited oxygen supply. Designing raw materials, pyrolysis temperature, and synthesis methods play important roles in manipulating the desired elemental compositions, porosity, and surface-active area of biochar [11], [12], [13], [14]. Biochar possesses a hierarchical porous structure including micropores, mesopores, and macropores. The hierarchical porous structure contributes greatly to the porosity and its surface-active area [15], [16], [17], [18]. The existence of the hierarchical porous structure is the key to the applicability of biochar. Due to its porosity, biochar has been widely applied as a soil conditioning agent and as an adsorbent for wastewater [4], [5], [8].

In recent years, biochar has demonstrated fascinating applicability in construction materials [19], [20], [21]. The porous nature of biochar typically owns a highly functionalised surface which provides nucleation sites for chemical reactions [21], [22]. Biochar shows a high compatibility in a composite system involving cement [19], [23], asphalt [20], [24], and polymeric materials[25], [26], [27]. Incorporating biochar improves the functionality of the construction materials. Several studies found that biochar enhances the physical and mechanical properties of construction materials, including biochar-cement composites [19], [28], biochar asphalt composites[20], [24], and biochar-plastic composites [25], [27]. Recent studies show that incorporating biochar in concrete composites influences the workability, hydration, and mechanical properties [28], [29], [30]. Some researchers found that not only the porosity but also the elemental compositions of biochar dictate its applicability. For instance, a calcium-rich biochar containing high $CaCO_3$ can be involved in the hydration process of cement [28], [31], [32], [33]. Therefore, the calcium-rich biochar can be a partial substitute for cement and can reduce the overall cost. On the other hand, calcium-poor biochar is suitable for filler aggregate in concrete or paver. In this case, employing biochar as aggregates helps to improve the ecosystem from the over-extraction of natural aggregates such as sand and gravel [21], [29].

Implementing biochar as a paving material has been shown to strengthen the paving structures. Previous studies assessed the optimation of run-off rainfall water absorption by incorporating biochar in the construction of permeable pavement. The addition of biochar can be used to regulate water absorbency and permeability of the paving to minimize puddles and flooding during the rainy season [23], [34]. Pervious concrete with biochar addition displays an increase in compressive or flexural strength. However, the compressive strength will be compromised if the biochar content exceeds a certain amount [30], [35], [36].

Indonesia is known as the world's largest producer of coconut and generates more than 0.75 million tons of coconut shell waste [14]. Coconut shells contain a high percentage of lignin, cellulose, and hemicellulose which can yield biochar with high carbon content. Determining a suitable pyrolysis temperature for the synthesis of coconut-shell biochar is essential to obtain the highest porosity. In this study, we investigate the coconut shell biomass waste as the raw material of biochar and the potential application of biochar as a permeable pavement. The novelty of this study is elucidating the direct connection between coconut-shell biochar, pyrolysis temperature, and the application as a permeable paving block based on its chemical and physical properties. The porosity and elemental compositions of the biochar were observed at temperatures 400°C and 500°C. The obtained biochar at an optimum temperature was used as a composite material of permeable pavement. The mechanical properties of the permeable pavement were studied based on the mass ratio of aggregate to biochar. The experimental results then were analyzed and compared to obtain the best quality of pavement based on SNI (The Indonesian National Standard).

2. Experimental Details

2.1. Materials

Coconut shell waste was obtained from a local agricultural waste disposal in Malang City, Indonesia. Fine aggregates were purchased from a local distributor. Cement Portland type 1 was purchased from Semen Gresik.

2.2. Pyrolysis of coconut-shell biochar

The coconut shells were cut and then dried under sunlight for 48 hours. After that, the dried coconut shells were pyrolyzed at temperatures of 400°C and 500°C in oxygen oxygen-limited environment for 1 h. Then, the pyrolyzed coconut shells were ball-milled for 15 min at 25 rpm. The total surface area and pore distribution were analyzed by N_2 desorption/adsorption isotherms obtained with Quantachrome Autosorb-iQ. In addition, the surface morphology and chemical compositions of the biochar were characterized by SEM-EDX (Scanning Electron Microscopy-Energy Dispersive X-ray Spectroscopy, FEI, Type: Inspect-S50).

2.3. The fabrication of permeable paver

Permeable paving was fabricated by mixing water, fine aggregates, Portland cement, and ball-milled biochar. The fine aggregates were characterized with ASTM C33 parameters to fulfil the specification of concrete aggregates. In the process, the weight and density of the fine aggregates were tested based on SNI 03-4804-1998 and SNI 1970:2008. The mass ratio of fine aggregates to biochar in the permeable paver was varied into 1:0, 0.8:0.2, 0.6:0.4, 0.4:0.6, 0.2:0.8, and 0:1. The sample label was abbreviated based on the biochar percentage, into $B_{0\%}$, $B_{20\%}$, $B_{40\%}$, $B_{60\%}$, $B_{80\%,}$ and $B_{100\%}$, respectively.

Dry mix and mechanical pressure were applied for the fabrication of permeable paving blocks. The biochar obtained from optimum pyrolysis temperature was employed to substitute fine aggregates. The sample preparation used a design mix with a ratio of cement to the total of fine aggregates and biochar 1:6. The samples were prepared by mixing all the materials and then poured into a sample mould with the dimensions of 5cmx5cmx5cm. To obtain valid data analysis and conclusions for water permeability and compressive test, six samples were prepared for one variation of biochar percentage. In total, 36 samples of permeable paving blocks were prepared and then characterized with compressive test and water absorption capacity after 28 days of curing time. The test results were analysed and compared to the standard for paving block SNI 03-0691-1996.

3. Results and Discussion

In this study, we utilized coconut shell waste into biochar by pyrolyzing it at temperatures 400°C and 500°C in an O_2-deprived condition. The biochar samples were abbreviated as B-400 and B-500, respectively. Before the pyrolysis, the coconut shell waste was treated by drying under sun rays to minimize the water content. The chosen pyrolysis temperatures were 400°C and 500°C because the pyrolysis temperature should be higher than the degradation temperature of hemicellulose (220-315°C), cellulose (315-400°C), and lignin (160-900°C) [37]. The hemicellulose, cellulose, and lignin are the major components of coconut shell waste. Lignin degrades at a wide range temperature and produces a high carbon residue reaching 40 wt% [38]. Porous structure in biochar was initiated by the removal of remaining moisture and volatile compounds. The thermal degradation of cellulose, hemicellulose, and lignin leads to a porous formation in the biochar. At a temperature higher than 200°C, the degradation of hemicellulose started, then followed by cellulose as the pyrolysis temperature increased. The remaining carbon residue most likely originated from lignin [23], [37]. However, this study limits the maximum pyrolysis temperature to 500°C. The reason is that the hydrophilicity of the biochar pyrolyzed at temperatures higher than 500°C decreased significantly. A highly hydrophobic biochar would be a drawback for the fabrication of permeable paver [39], [40].

The porous structure in biochar is essential to increase the water permeability of biochar for the application of permeable pavement. After the preparation of biochar was completed, the porosity and pore size distribution were characterized by N_2 desorption/adsorption isotherms and SEM-EDX to obtain an optimum pyrolysis temperature. The optimum temperature condition for biochar was selected based on the results of surface-active area and porosity. The purpose is that the biochar with a high surface area allows high water permeability when mixed in the fabrication of a permeable paver. Furthermore, the elemental compositions of the biochar were examined to know the effect of carbon content, water permeability, and the role of biochar in the fabrication of permeable paver. This study is expected to bring a better understanding of the correlation between pyrolysis temperature, surface active area, elemental compositions, and water permeability of biochar and its application as a permeable paving block.

Firstly, the surface morphology of B-400 and B-500 was characterized by SEM as shown in Fig. 1. Both B-400 and B-500 display a typical shape of monolith carbon [15], [16]. The high magnification of the SEM Figures 1b and 1d shows that the B-500 possesses a more uniform pore distribution than the B-400. A closer examination of the SEM figures b and d clearly shows that the porous structure of B-500 is deep, large, and interconnected into the inner structure of the biochar. The SEM results suggested that the B-500 might have a higher surface-active area than the B-400. The N_2 desorption/adsorption isotherm characterization with the BET (Brunauer-Emmett-Teller) method was carried out to know the surface-active area and pore size distribution quantitatively.

Surface active area and porosity analyses as the results of the BET method were displayed in Fig. 2 a and b. The N_2 desorption/adsorption isotherms of the B-400 (denoted as black line-symbol) and B-500 (denoted as red line-symbol) show a type I adsorption isotherm. The type I adsorption isotherm is commonly known as a pseudo-Langmuir isotherm, which depicts monolayer adsorption. The type I isotherm is obtained when the partial pressure, $P/P_o < 1$ and constant > 1 in

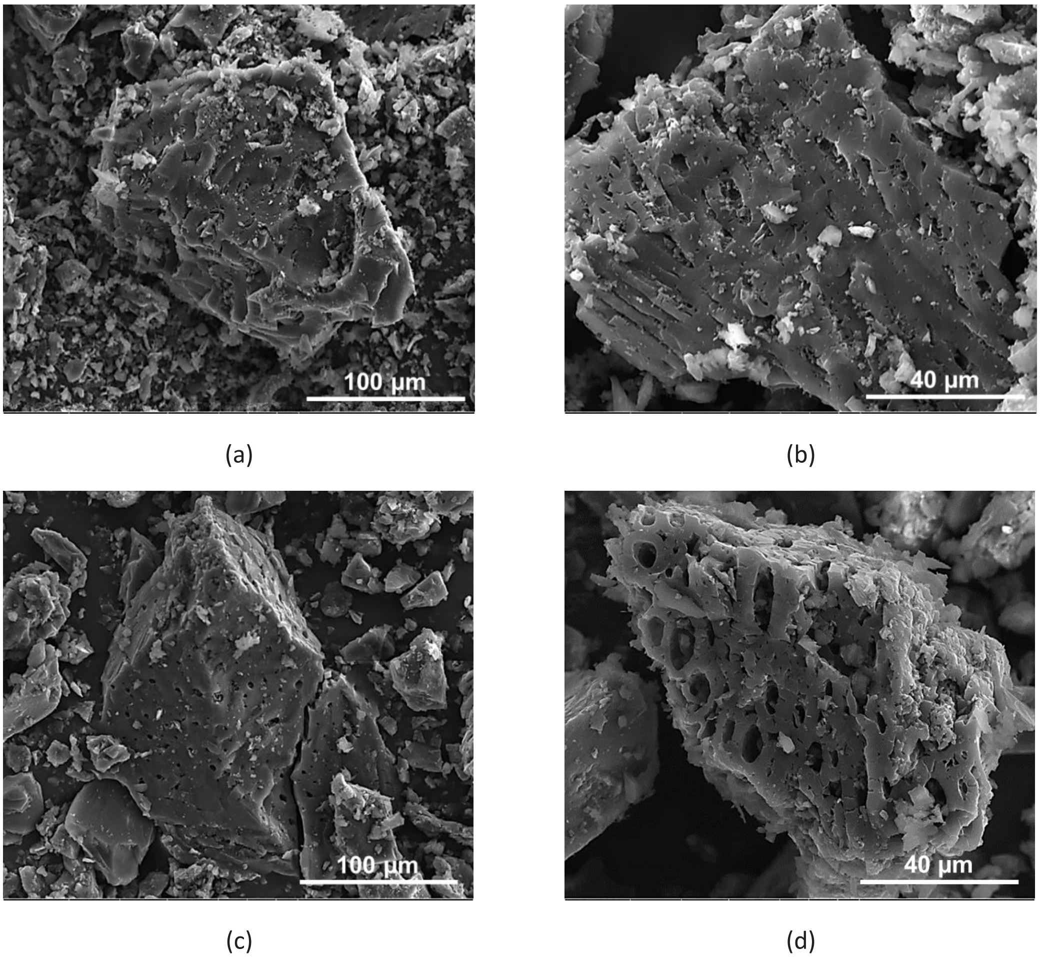

Fig. 1- Scanning Electron Microscope (SEM) of the coconut-waste biochar pyrolyzed at (a, b) 400 ℃ and (c, d) 500 ℃. The (a) and (b) were captured at a low magnification. The (b) and (d) were captured at a high magnification.

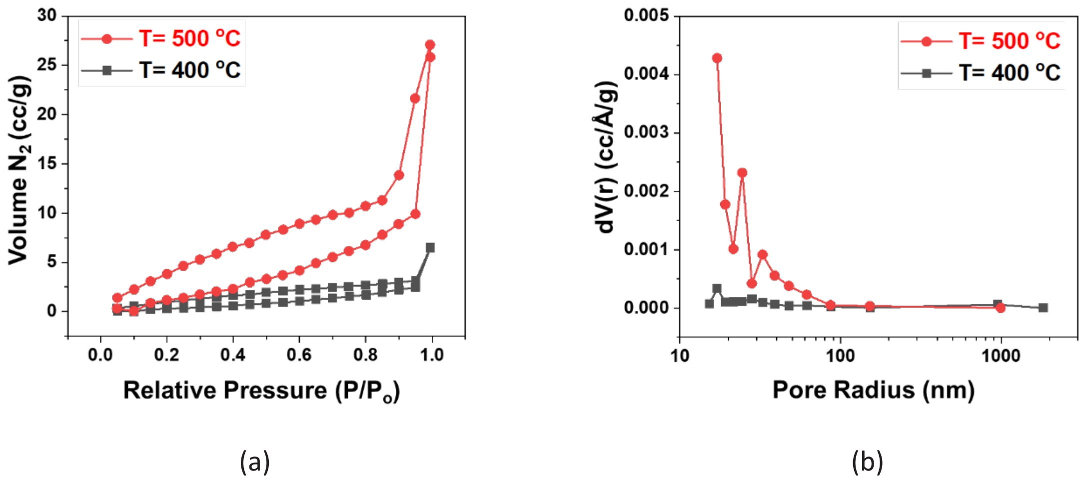

Fig. 2- (a) Nitrogen desorption/adsorption isotherms and (b) Pore size distribution of the coconut-waste biochar pyrolyzed at 400 ℃(black line-symbol) and 500 ℃ (red line-symbol).

the BET equation. Furthermore, as shown in Fig. 2a, the N_2 volumes of B-400 and B-500 display a hysteresis at 0.85 and close to 1, respectively. Both also display a steep increase in N_2 adsorption or a decrease in N_2 desorption/adsorption at a high P/P_o range. The results indicate that the porous structures of B-400 and B-500 are dominated by micropores.

The pore size distribution was demonstrated through the BJH (Barrett-Joyner-Halenda) analyses as shown in Fig. 2b. The pore size distribution of B-400 is dominated by micropores with an average diameter of 17 Å= 1.7 nm and the total surface-active area of the biochar is 3.573 m^2/g. On the other hand, the average pore size distribution of B-500 is 1.7 nm with a total surface-active area of 32.565 m^2/g. Both B-400 and B-500 have relatively similar average pore size distributions, namely 1.7 nm. However, the total surface-active area of B-500 is higher than B-400. This significant difference in the total surface-active area indicates that the pyrolysis temperature of 500°C is the optimum temperature for the thermal degradation of lignin, cellulose, and hemicellulose of the coconut shell waste. Based on the correlation of the BET results and the SEM figures, the pyrolysis temperature at 500°C produces a uniform pore distribution throughout the entire surface of the biochar. Moreover, the pore structure also penetrates the inner part of the biochar which produces an interconnected structure. The uniform pore distribution at the surface area and interconnected pore structure in the inner part of the biochar resulting a high surface-active area.

The results of SEM and BET indicate that 500°C is the optimum pyrolysis temperature because the B-500 possesses a high porosity and total surface-active area. The porosity is an important parameter for the fabrication of permeable pavement since the porosity is directly linked to water permeability. Based on the porosity analyses, the B-500 is more suitable to be utilized as a composite material for permeable pavement.

Before the sample preparation of the permeable pavement, the elemental composition of the B-500 SEM-EDX was characterized. The purpose is to know the carbon content of the biochar since the carbon content influences the water-holding capacity. Previous studies show that high carbon content from biochar increases the water-holding capacity [9], [29]. Other studies state that the high water-holding capacity reduces the mechanical strength of concrete materials [8], [29], [30].

The result of SEM-EDX shows that the B-500 consists of 93.8% carbon, 5.9% oxygen, 0.1% silica, 0.1% aluminium, 0,1% sodium, and 0.1% potassium. Since 93.8% of the B-500 is comprised of carbon, an optimum mass ratio of biochar (B-500) used in the fabrication of permeable pavement should be determined. To be noted, B-500 is composed of only 0.1% silica and 0.1% aluminium. The small amount of Si, Al, and lack of calcium (Ca) implies that B-500 is not involved in the cement hardening process. The B-500 only can be utilized as a substitute for aggregates in the mixture of permeable paving.

Parameters of SNI-03-0691-1996, including compression strength and water permeability, were used to determine the optimum mass ratio of B-500 in the mixture of permeable pavement. The mass ratio of fine aggregates to biochar in the permeable paving was varied into 1:0, 0.8:0.2, 0.6:0.4, 0.4:0.6, 0.2:0.8, and 0:1. Six samples for each biochar ratio were prepared to obtain valid results on compression strength and water permeability tests. The sample label was abbreviated based on the biochar percentage, into $B_{0\%}$, $B_{20\%}$, $B_{40\%}$, $B_{60\%}$, $B_{80\%}$, and $B_{100\%}$, respectively. The prepared samples of paving blocks are shown in Fig. 3.

Fig. 3a shows the side view photograph of the prepared biochar paving blocks. From the visual observation, it is visible that the surface texture of the paving block without biochar ($B_{0\%}$) is smooth. The increase of biochar percentage in the paving blocks increases the surface roughness. In addition, the paving blocks of $B_{80\%}$ and $B_{100\%}$ were easily deformed. The compression strength and water permeability of the permeable paving blocks were tested. Figure 4a displays the compression strength results of the samples based on the varied biochar percentages. In the absence of B-500 ($B_{0\%}$), the paving block achieved the highest compression strength 41,2 MPa, and the lowest water permeability 0.62%. Based on the SNI-03-0691-1996, the $B_{0\%}$ is qualified to be used as a grade A paving block. Grade A paving block can be used as a construction for the main road. The composition of $B_{0\%}$ is similar to the commercial paving blocks. The result implies that indeed, the common paving block ($B_{0\%}$) shows high compression strength and, thus has a versatile and long-term application. However, the water permeability percentage of $B_{0\%}$ is close to 0%. The impermeable paving block can cause flooding during the peak rainy season. The application of impermeable paving block ($B_{0\%}$) will disrupt the natural water cycle by inhibiting rainwater to replenish aquifers. Furthermore, the poor drainage system and constant flooding can reduce the durability of paving blocks [41].

The addition of biochar reduces compression strength and inversely increases the water permeability as shown in Fig. 4 a and b. At $B_{20\%}$, the compression strength is reduced to 24.7 MPa with the water permeability of 6%. The $B_{20\%}$ is eligible for the grade B paving block. Grade B can be used as the construction material of a parking area. However, increasing the mass percentage of B-500 to $B_{40\%}$,

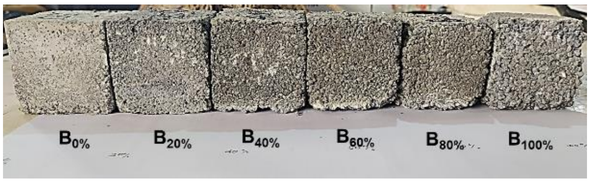

(a)

(b)

Fig. 3- Photographs of permeable paving mixed with coconut-waste biochar pyrolyzed at 500 ℃. The weight percentage of the biochar was varied at 0%, 20%, 40%, 60%, 80%, and 100%.

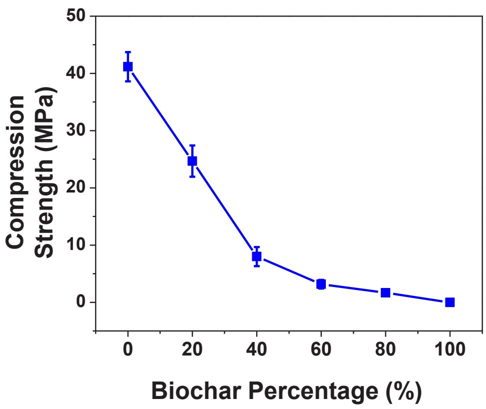

(a)

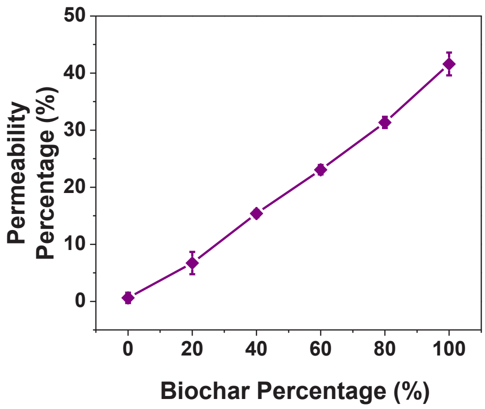

(b)

Fig. 4- (a) Compression strength and (b) Permeability percentage of permeable paving block mixed with a varied mass percentage of biochar $B_{0\%}$, $B_{20\%}$, $B_{40\%}$, $B_{60\%}$, $B_{80\%}$, and $B_{100\%}$, respectively.

$B_{60\%}$, $B_{80\%}$, and B_{100} decreases the compression strength and increases water permeability, causing it to be no longer adequate for paving block application. The reason is that the porous structure originating from biochar pyrolyzed at high temperatures is hygroscopic [30]. Increasing the mass percentage of B-500 in the mixture of paving blocks increases porosity. Since the porous structure is hygroscopic, the atmospheric water is easily bound to the pore surface of the B-500. The bound water can accumulate in the channel inside the porous structure of the paving block, resulting in clumpy biochar-cement aggregates. The clumpy biochar-cement aggregates are fragile and, hence inapplicable for paving block application. Based on the test results of compression strength and water permeability, the $B_{20\%}$ is regarded as the optimum mass percentage of biochar in the mixture for the production of permeable pavement.

This investigation can be used as a basis evaluation for the application of coconut biochar for construction materials, especially paving blocks. In the practical application, cost evaluation is essential for predicting the desirability and applicability of the permeable pavement. In this case, the $B_{20\%}$ has a high potential for a large-scale application. By adding 20wt% of biochar, the amount of fine aggregate can be reduced. In the large-scale application, reducing fine aggregates can have a positive impact on the environment. Reducing the amount of fine aggregate will decrease the use of natural aggregates, thus minimizing environmental damage. Compared to the cost of environmental damage caused by the exploitation of the natural aggregate, biochar is seen to be more cost-effective. Moreover, the incorporation of biochar as the partial substitute for fine aggregates of permeable pavement is considered cost-effective since its raw material originated from coconut shell waste. Moreover, a comprehensive cost analysis is still required since many factors are involved in the economic feasibility such as location, raw material price, and production technologies [42].

4. Conclusions

This work investigates the direct connection between the fabrication of biochar from coconut shell waste, pyrolysis temperature, and the application of biochar as a permeable paving block. The connection was closely examined based on chemical and physical properties. Two pyrolysis temperatures of biochar, 400°C and 500°C were carried out. Indeed, the pyrolysis temperature plays an important role in the porosity of biochar. The degradation of lignin, hemicellulose, and cellulose at 500°C produces a prominent porous structure that penetrates deep inside the B-500, resulting in a total surface-active area of 32.565 m^2/g. The B-500 achieved a significantly higher surface-active area than B-400 which is only 3.573 m^2/g. The lack of Si, Al, and Ca in the elemental composition of B-500 implies that the biochar is not involved in the cement hardening process. The role of B-500 is as a substitute for aggregates in the mixture of permeable paving. Adding B-500 to the mixture of paving blocks affects the compression strength and water permeability due to the hygroscopic property of B-500. The $B_{20\%}$ which consists of 20% biochar is adequate to be utilized as a grade B paving block based on The Indonesian National Standard (SNI). At $B_{20\%}$, the compression strength is 24.7 MPa and the water permeability is 6%. In future research, exploring a wider variety of pyrolysis temperatures, raw material and composite material of biochar are essential to achieve the optimum composite composition of permeable paving. The future-designed permeable pavement is expected to have better quality and long-term durability in various environmental conditions.

Acknowledgement

This research is made possible through monetary assistance of the internal funding (scheme B) by Institut Teknologi Nasional Malang. The authors are very thankful for the support, and facilities provided by the Department of Chemical Engineering and Civil Engineering of Institut Teknologi Nasional (ITN) Malang. In addition, the authors are also grateful for financial support from the Rumah Program of Research Organization of Nanotechnology and Materials (ORNM) year 2025 of the National Research and Innovation Agency (BRIN).

References

1. A. Moustafa, R. Elganainy, and S. Mansour, “Insights into the UNSG announcement: The end of climate change and the arrival of the global boiling era, July 2023 confirmed as the hottest month recorded in the past 120,000 years,” Catrina Int J Environ Sci, vol. 28, no. 1, pp. 43–51, Jul. 2023.
2. A. Twidyawati, Nurbani, W. B. Prasetyo, S. E. Manurung, and A. M. Pebriadi, “Adaptation and mitigation strategies for impacts and efforts of climate change in Indonesia,” IOP Conf Ser Earth Environ Sci, vol. 824, no. 1, p. 012092, Jul. 2021.
3. T. Amnuaylojaroen, “Perspective on the Era of Global Boiling: A Future beyond Global Warming,” Advances in Meteorology, vol. 2023, pp. 1–12, Dec. 2023.
4. M. Arif et al., “Biochar; a Remedy for Climate Change,” in Environment, Climate, Plant and Vegetation Growth, Cham: Springer International Publishing, 2020, pp. 151–171.
5. J. Lehmann et al., “Biochar in climate change mitigation,” Nat Geosci, vol. 14, no. 12, pp. 883–892, Dec. 2021.
6. R. Aryapratama and S. Pauliuk, “Life cycle carbon emissions of different land conversion and woody biomass utilization scenarios in Indonesia,” Science of The Total Environment, vol. 805, p. 150226, Jan. 2022.
7. D. S. Adetama, A. Fauzi, B. Juanda, and D. B. Hakim, “A Policy Framework and Prediction on Low Carbon Development in the Agricultural Sector in Indonesia,” International Journal of Sustainable Development and Planning, vol. 17, no. 7, pp. 2209–2219, Nov. 2022.

8. D. K. Gupta et al., "Role of Biochar in Carbon Sequestration and Greenhouse Gas Mitigation," in Biochar Applications in Agriculture and Environment Management, Cham: Springer International Publishing, 2020, pp. 141–165.
9. L. Luo et al., "Carbon Sequestration Strategies in Soil Using Biochar: Advances, Challenges, and Opportunities," Environ Sci Technol, vol. 57, no. 31, pp. 11357–11372, Aug. 2023.
10. S. Gupta and H. W. Kua, "Factors Determining the Potential of Biochar As a Carbon Capturing and Sequestering Construction Material: Critical Review," Journal of Materials in Civil Engineering, vol. 29, no. 9, Sep. 2017.
11. W. A. Rizal et al., "Coconut Shell Waste Treatment Technology for A Sustainable Waste Utilization: A Case Study of the SMEs in Bohol Village, Indonesia," ASEAN Journal of Community Engagement, vol. 6, no. 2, Dec. 2022.
12. R. Kabir Ahmad, S. Anwar Sulaiman, S. Yusup, S. Sham Dol, M. Inayat, and H. Aminu Umar, "Exploring the potential of coconut shell biomass for charcoal production," Ain Shams Engineering Journal, vol. 13, no. 1, p. 101499, Jan. 2022.
13. M. Tripathi, J. N. Sahu, and P. Ganesan, "Effect of process parameters on production of biochar from biomass waste through pyrolysis: A review," Renewable and Sustainable Energy Reviews, vol. 55, pp. 467–481, Mar. 2016.
14. A. Tomczyk, Z. Sokołowska, and P. Boguta, "Biochar physicochemical properties: pyrolysis temperature and feedstock kind effects," Rev Environ Sci Biotechnol, vol. 19, no. 1, pp. 191–215, Mar. 2020.
15. C. M. Septani, C. A. Wang, U. S. Jeng, Y. C. Su, B. T. Ko, and Y. Sen Sun, "Hierarchically Porous Carbon Materials from Self-Assembled Block Copolymer/Dopamine Mixtures," Langmuir, vol. 36, no. 40, pp. 11754–11764, Oct. 2020.
16. C. M. Septani, C.-C. Wang, and Y.-S. Sun, "Oxygen Reduction Reaction of Block Copolymer Template-Directed Porous Carbon Catalysts," ACS Appl Energy Mater, vol. 5, no. 1, pp. 897–914, Jan. 2022.
17. C.-H. Sun, C. M. Septani, and Y.-S. Sun, "Direct Access to Bowl-Like Nanostructures with Block Copolymer Anisotropic Truncated Microspheres," Langmuir, vol. 37, no. 2, pp. 636–645, Jan. 2021.
18. N. A. Rahman, M. Ajiza, and C. M. Septani, "Aerogel sensoric nanoparticles with controlled surface area and pore structure synthesized from bagasse ash," 2024, p. 030005.
19. C. Labianca et al., "A holistic framework of biochar-augmented cementitious products and general applications: Technical, environmental, and economic evaluation," Environ Res, vol. 245, p. 118026, Mar. 2024.
20. N. S. A. Yaro et al., "A Comprehensive Review of Biochar Utilization for Low-Carbon Flexible Asphalt Pavements," Sustainability, vol. 15, no. 8, p. 6729, Apr. 2023.
21. Y. Zhang et al., "Biochar as construction materials for achieving carbon neutrality," Biochar, vol. 4, no. 1, p. 59, Dec. 2022.
22. G. Habert et al., "Environmental impacts and decarbonization strategies in the cement and concrete industries," Nat Rev Earth Environ, vol. 1, no. 11, pp. 559–573, Sep. 2020.
23. S. Gupta, H. W. Kua, and H. J. Koh, "Application of biochar from food and wood waste as green admixture for cement mortar," Science of The Total Environment, vol. 619–620, pp. 419–435, Apr. 2018.
24. H. A. Rondón-Quintana, F. A. Reyes-Lizcano, S. B. Chaves-Pabón, J. G. Bastidas-Martínez, and C. A. Zafra-Mejía, "Use of Biochar in Asphalts: Review," Sustainability, vol. 14, no. 8, p. 4745, Apr. 2022.
25. Y. Bai, A. Arulrajah, S. Horpibulsuk, and A. Zhou, "Geopolymer stabilization of carbon-negative gasified olive stone biochar as a subgrade construction material," Constr Build Mater, vol. 442, p. 137617, Sep. 2024.
26. A. N. F. Ganda et al., "Utilization of Banana Peels as Biopolymer Nanocomposites: A Preliminary Study on the Addition of Electrochemically Exfoliated Graphene," Journal of Ultrafine Grained and Nanostructured Materials, vol. 57, no. 2, pp. 120–127, 2024.
27. F. Piccolo, F. Andreola, L. Barbieri, and I. Lancellotti, "Synthesis and Characterization of Biochar-Based Geopolymer Materials," Applied Sciences, vol. 11, no. 22, p. 10945, Nov. 2021.
28. X. Lin, W. Li, Y. Guo, W. Dong, A. Castel, and K. Wang, "Biochar-cement concrete toward decarbonisation and sustainability for construction: Characteristic, performance and perspective," J Clean Prod, vol. 419, p. 138219, Sep. 2023.
29. L. Chen et al., "Biochar-augmented carbon-negative concrete," Chemical Engineering Journal, vol. 431, p. 133946, Mar. 2022.
30. K. Tan, Y. Qin, T. Du, L. Li, L. Zhang, and J. Wang, "Biochar from waste biomass as hygroscopic filler for pervious concrete to improve evaporative cooling performance," Constr Build Mater, vol. 287, p. 123078, Jun. 2021.
31. X. Yang and X.-Y. Wang, "Strength and durability improvements of biochar-blended mortar or paste using accelerated carbonation curing," Journal of CO2 Utilization, vol. 54, p. 101766, Dec. 2021.
32. S. Kushwah et al., "Mixture of biochar as a green additive in cement-based materials for carbon dioxide sequestration," Journal of Materials Science: Materials in Engineering, vol. 19, no. 1, p. 27, Sep. 2024.
33. D. Winters, K. Boakye, and S. Simske, "Toward Carbon-Neutral Concrete through Biochar–Cement–Calcium Carbonate Composites: A Critical Review," Sustainability, vol. 14, no. 8, p. 4633, Apr. 2022.
34. R. Walters, S. A. Begum, E. H. Fini, and T. M. Abu-Lebdeh, "Investigating Bio-Char as Flow Modifier and Water Treatment Agent for Sustainable Pavement Design," American Journal of Engineering and Applied Sciences, vol. 8, no. 1, pp. 138–146, Jan. 2015.
35. C. Xie, L. Yuan, H. Tan, Y. Zhang, M. Zhao, and Y. Jia, "Experimental study on the water purification performance of biochar-modified pervious concrete," Constr Build Mater, vol. 285, p. 122767, May 2021.
36. K. Tan, Y. Qin, T. Du, L. Li, L. Zhang, and J. Wang, "Biochar from waste biomass as hygroscopic filler for pervious concrete to improve evaporative cooling performance," Constr Build Mater, vol. 287, p. 123078, Jun. 2021.
37. H. Yang, R. Yan, H. Chen, D. H. Lee, and C. Zheng, "Characteristics of hemicellulose, cellulose and lignin pyrolysis," Fuel, vol. 86, no. 12–13, pp. 1781–1788, Aug. 2007.
38. D. Watkins, Md. Nuruddin, M. Hosur, A. Tcherbi-Narteh, and S. Jeelani, "Extraction and characterization of lignin from different biomass resources," Journal of Materials Research and Technology, vol. 4, no. 1, pp. 26–32, Jan. 2015.
39. J. Mao, K. Zhang, and B. Chen, "Linking hydrophobicity of biochar to the water repellency and water holding capacity of biochar-amended soil," Environmental Pollution, vol. 253, pp. 779–789, Oct. 2019.
40. A. Tomczyk, Z. Sokołowska, and P. Boguta, "Biochar physicochemical properties: pyrolysis temperature and feedstock kind effects," Rev Environ Sci Biotechnol, vol. 19, no. 1, pp. 191–215, Mar. 2020.
41. M. Ghavanloughajar et al., "Compaction conditions affect the capacity of biochar-amended sand filters to treat road runoff," Science of The Total Environment, vol. 735, p. 139180, Sep. 2020.
42. M. B. Ahmed, J. L. Zhou, H. H. Ngo, and W. Guo, "Insight into biochar properties and its cost analysis," Biomass Bioenergy, vol. 84, pp. 76–86, Jan. 2016.